SIAM J. APPL. MATH.
Vol. 61, No. 1, pp. 213–231

AN ENVELOPE METHOD FOR ANALYZING SEQUENTIAL PATTERN FORMATION*

GERHARD C. CRUYWAGEN†, PHILIP K. MAINI‡, AND JAMES D. MURRAY§

Abstract. We examine sequential spatial pattern formation in a tissue interaction model for skin organ morphogenesis. Pattern formation occurs as a front sweeps across the domain leaving in its wake a steady state spatial pattern. Extensive numerical simulations show that these fronts travel with constant wave speed. By considering the envelope of the solution profile we present a novel method of calculating its wave speed.

Key words. pattern formation, envelope method, sequential pattern formation, wave speed, tissue interaction

AMS subject classifications. 92, 35

PII. S003613999732857X

1. Introduction.

The vast range of patterns and structures observed in animals develops from the apparently homogeneous mass of cells that constitutes the early embryo. In an attempt to understand the underlying mechanisms of this process, termed morphogenesis, mathematical modeling has been used extensively.

Most mathematical models for morphogenesis focus on synchronous pattern formation (see Murray (1989) for a review). However, morphogenetic processes frequently occur sequentially. Regular patterns of repeated units often develop at a frontier of pattern formation (Zeeman (1974)) which moves across the prospective area to transform unstructured tissue into an array of patterned components.

A typical example of sequential skin pattern formation is in the chick embryo where feather germ initiation occurs sequentially, row by row, with the first row being laid down on the dorsal midline (Davidson (1983a), (1983b)). Similar waves of pattern formation also occur, for example, in the development of somites (Pearson and Elsdale (1979)), scales (Maderson (1965a), (1965b)), and alligator skin patterns (Murray, Deeming, and Ferguson (1990)).

Recently, Cruywagen and Murray (1992) proposed a novel tissue interaction model for describing skin patterning. As was demonstrated by Cruywagen and Murray (1992) and Cruywagen, Maini, and Murray (1997), their tissue interaction model can account for synchronous patterning. The model can also exhibit propagating patterns. For example, Cruywagen, Maini, and Murray (1992) showed that the model, solved on a rectangular domain, can exhibit propagating patterns resulting in stripes, consistent with patterns observed in the developing alligator embryo, or rhombic structures, consistent with those observed during feather germ formation on embryonic dorsal chick skin. In both of these cases, sequential pattern formation resulted from a small lo-

*Received by the editors October 8, 1997; accepted for publication (in revised form) March 30, 1999; published electronically July 5, 2000.
http://www.siam.org/journals/siap/61-1/32857.html
†Sea Fisheries Research Institute, Private Bag X2, Rogge Bay, 8012 Cape Town, South Africa (gcruywag%boland@mus.cstat.co.za).
‡Centre for Mathematical Biology, Mathematical Institute, 24–29 St. Giles', Oxford, UK (maini@maths.ox.ac.uk).
§Department of Applied Mathematics, Box 352420, University of Washington, Seattle, WA 98195 (murrayjd@amath.washington.edu). This author's work was supported in part by National Science Foundation grant DMS 9500766 and National Institutes of Health grant 2P41-RR-01243-12.

calized disturbance in the tissue which developed into a pattern and subsequently propagated through the domain as a *traveling wave* of pattern formation.

The phenomenon of traveling waves occurs throughout nature (Maini (1995), (1996)) and has been widely studied. In most cases the wave sweeps across the domain as the variable switches from one unstable, homogeneous steady state to another stable, uniform steady state. Such models were first studied by Fisher (1937) and Kolmogoroff, Patrovsky, and Piscounoff (1937), who showed how to determine the wave speed of the front by first transforming to traveling wave coordinates.

The traveling waves that we investigate in this paper are rather different because they consist of a traveling front that leaves in its wake a *spatially* varying steady state solution. Myerscough and Murray (1992) analyzed such traveling waves for a cell-chemotaxis model and used the method of steepest descents to find the speed of the traveling front. In this paper, we propose a new method, using *envelope* functions, for determining the wave speed of such propagating patterns. This method is valid in the vicinity of the bifurcation point from the homogeneous steady state solutions to patterned steady state solutions.

In section 2 we briefly describe the basic tissue interaction model of Cruywagen and Murray (1992) which we believe is currently one of the more biologically realistic models for pattern formation. Using linear analysis, we delimit regions in a parameter space where the uniform steady state of this system is unstable and, using a weakly nonlinear analysis, we determine, analytically, the spatially varying pattern to which the solutions evolve.

In section 3 we demonstrate that sequential pattern formation can be induced by a small localized disturbance in the tissue, which subsequently develops into a spatially varying pattern that propagates through the domain. A crucial observation is that the envelope of the solutions exhibits a traveling wave-like behavior from one spatially *uniform* state to another. We exploit this behavior in section 4 to generalize the Fisher-type analysis to such traveling waves. In section 5 we illustrate the application of this method by considering a specific example. It is important to note that this method is applicable in general to all pattern formation models that exhibit such traveling wave behavior. We use the tissue interaction model here merely by way of example.

2. Model equations. Vertebrate skin is composed of two layers—the epidermis and the dermis. Skin organ formation typically occurs due to interaction between these two layers. For example, in chick skin a feather germ arises as a result of tissue interaction leading to an aggregation of dermal cells, termed a papilla, underlying a thickening in the epidermis, termed a primordium. The model we consider here consists of two coupled equations, one for each layer. A crucial aspect of the biology captured by this model is that the pattern can only occur as a result of *both* layers interacting with one another. (For a discussion of modeling tissue interaction in general, see Murray and Cruywagen (1994) and Murray, Cruywagen, and Maini (1994).)

Here we consider a reduced tissue interaction model. Details of the full model can be found in Appendix A of this paper, and Cruywagen and Murray (1992). Cruywagen, Maini, and Murray (1997) show that this reduced model captures the salient features of the full model.

The reduced model focuses on the two key field variables—$\theta(x,t)$, which represents the epithelial dilation, and $n(x,t)$, which is the dermal cell density at position x (we are considering the one-dimensional case only) and time t.

The nondimensionalized model is

$$\overbrace{\mu\frac{\partial^3\theta}{\partial t\partial x^2}+\frac{\partial^2\theta}{\partial x^2}-\beta\frac{\partial^4\theta}{\partial x^4}}^{\text{effects of passive forces}}+\overbrace{\frac{\partial^2}{\partial x^2}\left\{\frac{\tau n^2}{[1+\nu(1-\theta)]^2+cn^2}\right\}}^{\text{active traction}}=\overbrace{\rho\theta}^{\text{body forces}}, \tag{2.1a}$$

$$\frac{\partial n}{\partial t}=\overbrace{D\frac{\partial^2 n}{\partial x^2}}^{\text{diffusion}}-\overbrace{\alpha\frac{\partial}{\partial x}\left\{n\frac{\partial}{\partial x}\left(\frac{1-\theta}{1+\gamma n}\right)\right\}}^{\text{chemotaxis}}+\overbrace{n(1-n)}^{\text{cell growth}}, \tag{2.1b}$$

where μ, β, τ, ν, c, ρ, D, α, and γ are positive parameters.

The tissue interaction in these caricature equations is represented in (2.1a) by the fourth term on the left-hand side, in which cell traction in the epidermis is a function of dermal cell density, and in (2.1b) by the second term on the right-hand side, in which dermal cell chemotaxis is a function of the dilation in the epidermis.

Equations (2.1) admit the spatially homogeneous steady states

$$n=0,\ \ \theta=0 \quad \text{and} \quad n=1,\ \ \theta=0.$$

Since we are interested in spatial pattern formation occurring in established cell populations, the trivial steady state is irrelevant. (For traveling wave solutions connecting the two steady states refer to Cruywagen, Maini, and Murray (1994).)

We linearize about the nontrivial steady state in the usual way to obtain the dispersion relation $\lambda(k^2)$ for the temporal growth of perturbations of wave number k as

$$\lambda(k^2)=\begin{cases}\dfrac{-b(k^2)+\Re\left(\sqrt{b^2(k^2)-4a(k^2)c(k^2)}\right)}{2a(k^2)} & \text{if } k^2\neq 0,\\ -r & \text{if } k^2=0,\end{cases} \tag{2.2}$$

where

$$\begin{aligned}a(k^2)&=\mu k^2,\\ b(k^2)&=(\mu D+\mu Q_1+\beta)k^4+(P_1+1+\mu r)k^2+\rho,\\ c(k^2)&=\beta(D+Q_1)k^6-(P_2Q_2-r\beta-DP_1-P_1Q_1-D-Q_1)k^4\\ &\quad+(r+rP_1+\rho D+\rho Q_1)k^2+\rho r,\end{aligned}$$

and

$$P_1=\frac{2\tau\nu(1+\nu)}{(1+2\nu+\nu^2+c)^2}, \tag{2.3a}$$

$$P_2=\frac{2\tau(1+2\nu+\nu^2)}{(1+2\nu+\nu^2+c)^2}, \tag{2.3b}$$

$$Q_1=\frac{\alpha\gamma}{(1+\gamma)^2}, \tag{2.3c}$$

$$Q_2=\frac{\alpha}{1+\gamma}. \tag{2.3d}$$

Spatially heterogeneous solutions of the linear system are characterized by a dispersion relation satisfying $\Re\lambda(0)\leq 0$ but which exhibits a range of modes corresponding to the eigenvalues $k^2>0$ with $\Re\lambda(k^2)>0$. In this case, the uniform steady state

is unstable to spatially heterogeneous perturbations, and these modes grow initially. As the amplitudes of these modes increase and the linear approximation is no longer valid, it is the form of the nonlinearities that is crucial in determining the final pattern. Cruywagen and Murray (1992) and Cruywagen, Maini, and Murray (1997) used extensive numerical simulation, steady state analyses, and weakly nonlinear bifurcation analyses to show that, in the vicinity of a primary bifurcation point, the linear stability analysis gives a very good indication as to the form of the solution of the full nonlinear problem.

In this paper, we consider a simplified version of the reduced model in which D, r, and μ are set equal to zero. This simplification is biologically realistic because the dermal cell diffusion effect is very small compared to the chemotactic term, cell proliferation appears to cease when pattern formation starts, and the epidermal viscosity coefficient is believed to be relatively very small. The parameter γ is used as the bifurcation parameter, with the critical value $\gamma = \gamma_c$ corresponding to the neutrally stable case for the homogeneous steady state; that is where $\lambda(k_c^2) = 0$ for a critical k_c^2. By setting $\gamma = \gamma_c - \epsilon^2$, where $\epsilon \ll 1$, the steady state becomes marginally unstable and a nonlinear perturbation analysis can be carried out (see Appendix B of this paper and Cruywagen and Murray (1992)). The general one-dimensional solution obtained on the infinite domain is

$$\begin{pmatrix}\theta\\ n\end{pmatrix} = \begin{pmatrix}0\\ 1\end{pmatrix} + \epsilon \begin{pmatrix}1\\ M\end{pmatrix} (A\cos k_c x + B \sin k_c x) + O(\epsilon^2) \text{ as } T \to \infty, \tag{2.4}$$

where $A^2 + B^2 = -\Gamma/\Omega$, with Ω and Γ complex expressions of the model parameters, $M = -(\gamma_c + 1)/\gamma_c$, and T is a slow timescale (see Appendix B).

3. Propagating patterns. Cruywagen and Murray (1992) solved the tissue interaction system on a one-dimensional spatial domain. As initial conditions they used random perturbations about the homogeneous steady states for the dermal cell density n and the epithelial dilation θ. This led to a pattern of peaks and troughs developing simultaneously across the whole domain. If, however, a perturbation is made in, say, the dermal cell density n in just one small region on a very large domain, the pattern is generated progressively. In effect the initial conditions, as specified in this case, give rise to a propagating wave of pattern.

This behavior can be illustrated by solving the simplified reduced model numerically. Figure 1 shows the solution obtained when the model is solved using the NAG FORTRAN routine D03PGF for the parameter set

$$\gamma_c = 1.0 - \epsilon^2, \qquad c = 1.0, \qquad \nu = 4.0, \qquad \alpha = 4.0,$$

$$\tau = 6.25, \qquad \beta = 0.011258, \qquad \rho = 88.826,$$

where γ_c is the bifurcation parameter and $\epsilon = 0.1$. The system was solved on the domain $[0, 30]$ with zero-flux boundary conditions. Initially n and θ were set to their respective homogeneous steady states, $\theta = 0$ and $n = 1$, on the whole domain, except for a small region at the origin. Here we specified small random perturbations about the steady state.

As expected these perturbations develop into a coherent spatial pattern which gradually propagates outward into the rest of the domain. The result is a traveling wave of pattern formation propagating from the origin toward the other end of the domain. Figure 1 illustrates how the pattern in dermal cell density progresses with

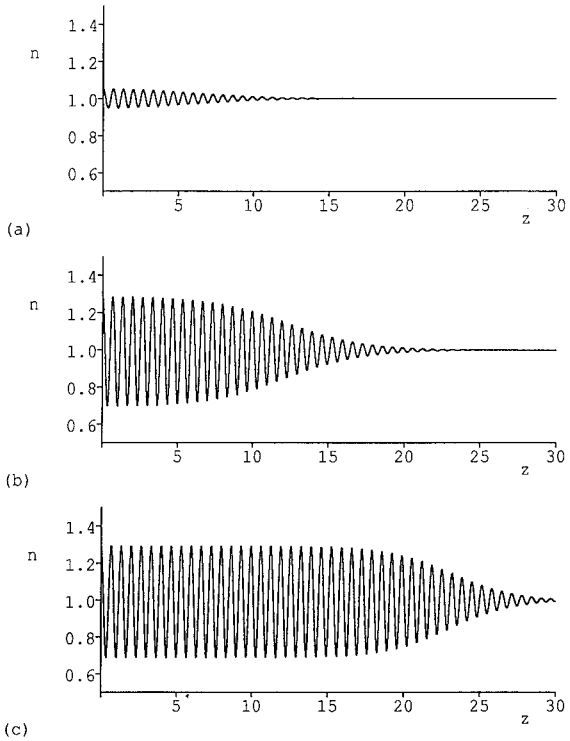

FIG. 1. *The time evolution of propagating patterns generated from random initial conditions at the origin by solving* (2.1) *with parameter values as shown in section* 3. (a) $t = 15$, (b) $t = 22$, *and* (c) $t = 29$.

time (since the pattern in dilation is similar to that for the dermal cell density, we only show the latter). This type of behavior is similar to that obtained by Myerscough and Murray (1992) for a reaction-diffusion–chemotaxis model.

Far away from the initial disturbance, the wavelength of the standing pattern and its speed of propagation seem to be constant and independent of the initial conditions. This motivates us to look for analytical methods to determine expressions for these quantities.

4. Envelope technique for propagating pattern analysis. By connecting the peaks and troughs of the evolving cell density and cell dilation patterns one can construct *envelopes* which enclose the developing patterns (see Figure 2(a)). It is crucial to note that these envelopes *travel* at the same speed as the propagating patterns. Here we use the properties of these envelopes to determine the approximate minimum wave speed of the spreading pattern.

We introduce a coordinate system moving with the traveling pattern by the usual change of variables $z = x - vt$, where v is a positive constant. We are thus concerned with patterns propagating in the positive x-direction. The assumption that the patterns travel at a constant speed v is based on the results of extensive numerical

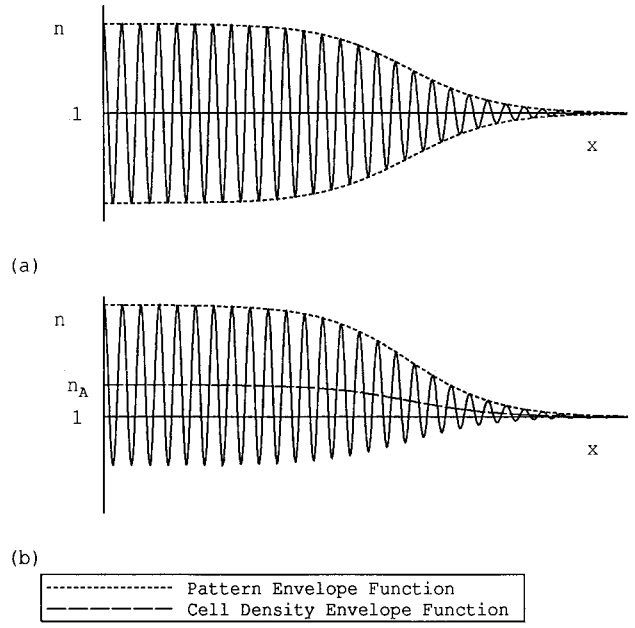

FIG. 2. (a) *An illustration of the* envelope *of the propagating wave of pattern formation in cell density.* (b) *An illustration of the envelope functions representing changes in the amplitude of the pattern and in the average cell density.*

simulations. The transformed system can be written in terms of x and z as

$$-\mu v\left(\frac{\partial^3\theta}{\partial z^3}+2\frac{\partial^3\theta}{\partial z^2\partial x}+\frac{\partial^3\theta}{\partial z\partial x^2}\right)+\left(\frac{\partial^2\theta}{\partial z^2}+2\frac{\partial^2\theta}{\partial z\partial x}+\frac{\partial^2\theta}{\partial x^2}\right)$$
$$-\beta\left(\frac{\partial^4\theta}{\partial z^4}+4\frac{\partial^4\theta}{\partial z^3\partial x}+6\frac{\partial^4\theta}{\partial z^2\partial x^2}+4\frac{\partial^4\theta}{\partial z\partial x^3}+\frac{\partial^4\theta}{\partial x^4}\right)$$
$$+\tau\left(\frac{\partial^2}{\partial z^2}+\frac{\partial^2}{\partial z\partial x}+\frac{\partial^2}{\partial x^2}\right)\left(\frac{n^2}{[1+\nu(1-\theta)]^2+cn^2}\right)=\rho\theta, \tag{4.1a}$$

$$-v\frac{\partial n}{\partial z}=D\left(\frac{\partial^2 n}{\partial z^2}+2\frac{\partial^2 n}{\partial z\partial x}+\frac{\partial^2 n}{\partial x^2}\right)+rn(1-n)$$
$$-\alpha\left(\frac{\partial}{\partial z}+\frac{\partial}{\partial x}\right)\left\{n\left(\frac{\partial}{\partial z}+\frac{\partial}{\partial x}\right)\left(\frac{1-\theta}{1+\gamma n}\right)\right\}, \tag{4.1b}$$

where θ and n are now functions of x and z.

We introduce three envelope functions: the envelope of the pattern in epithelial dilation; the envelope of the pattern in dermal cell density; and an "envelope" to represent the change in the average dermal cell density (see Figure 2(b)). We represent these by the normalized curves $p(z)$, $q(z)$, and $s(z)$, respectively. The last function $s(z)$ is, strictly speaking, not an envelope, but for convenience we shall describe it as

such. The following properties are ascribed to the envelope functions:

$$\lim_{z\to\infty} p(z) = 0, \quad \lim_{z\to\infty} q(z) = 0, \quad \lim_{z\to\infty} s(z) = 0, \tag{4.2a}$$

$$\lim_{z\to-\infty} p(z) = 1, \quad \lim_{z\to-\infty} q(z) = 1, \quad \lim_{z\to-\infty} s(z) = 1. \tag{4.2b}$$

We further assume that the solution of the system (4.1) can be expressed as

$$\theta(x,z) = p(z)\theta_G(x,z), \tag{4.3a}$$

$$n(x,z) = q(z)[n_G(x,z) - n_A] + s(z)(n_A - 1) + 1, \tag{4.3b}$$

where θ_G and n_G are functions that will be determined below. The value n_A is the average dermal cell density as $z \to -\infty$,

$$n_A = \lim_{z\to-\infty} \frac{1}{P}\int_0^P n(x,z)dx,$$

where P is the period of the steady state spatial pattern at $z = -\infty$.

The motivation for taking these solution forms comes from examination of the solutions illustrated in Figures 1 and 2, in which it is apparent that the solutions can be approximated very closely by a constant wavelength spatial pattern that has an amplitude that decreases monotonically. Note that the envelope function $s(z)$ appears in the expression for $n(x,z)$. This is because the average cell density, n_A, of the final solution is not necessarily equal to the initial average cell density $n = 1$, which is the homogeneous steady state value. So we have to track the change in average cell density, which is due to the logistic growth term in our dermal cell conservation equation, as well as the change in the developing pattern. In fact, in the simplified version of the model that will be considered below, the logistic growth term is set to zero and this envelope term disappears.

To determine the functions $n_G(x,z)$ and $\theta_G(x,z)$, we examine the solution behavior in the limit as $z \to \pm\infty$. Far behind the leading edge of the disturbance, that is, where $z \to -\infty$, the system is at a spatially periodic steady state, say S_1. We represent this steady state pattern by $S_1 = (\theta_{S_1}(x), n_{S_1}(x))^T$, which is also the solution of the z-independent nonlinear problem. So, from (4.2) and (4.3) it follows that

$$\lim_{z\to-\infty} \begin{pmatrix} \theta_G(x,z) \\ n_G(x,z) \end{pmatrix} = \begin{pmatrix} \theta_{S_1}(x) \\ n_{S_1}(x) \end{pmatrix}.$$

Far ahead of the leading edge of the disturbance, that is, as $z \to \infty$, the system is at the homogeneous steady state S_0, where $S_0 = (0,1)$. As the disturbance propagates into the homogeneous region, the steady state is perturbed and a spatially periodic solution begins to evolve. We represent the form of this initial pattern in dilation and cell density by the functions $\theta_{S_0}(x)$ and $n_{S_0}(x)$, respectively. In terms of the above expressions (4.2) and (4.3) this means that

$$\lim_{z\to\infty} \begin{pmatrix} \theta_G(x,z) \\ n_G(x,z) \end{pmatrix} = \begin{pmatrix} \theta_{S_0}(x) \\ n_{S_0}(x) \end{pmatrix}.$$

Additionally, we assume that the amplitudes of the periodic functions $\theta_{S_0}(x)$ and $n_{S_0}(x)$, representing the initial shape of the patterns, are the same as the amplitudes of the final pattern $\theta_{S_1}(x)$ and $n_{S_1}(x)$. The change in form of the initial pattern

at S_0 into the final pattern at S_1 is tracked by the functions $\theta_G(x,z)$ and $n_G(x,z)$. However, in the vicinity of a primary bifurcation from the uniform steady state, the most significant change in the patterns is in their amplitudes, while changes in their shapes are negligible in comparison (see Figure 1). Hence, we will assume that $\theta_G(x,z)$ and $n_G(x,z)$ are independent of z and thus that the final steady state pattern far behind the wave is the same shape as the initially evolving pattern at the leading edge of the wave, with the amplitudes tracked by the envelope functions. For notational convenience we shall write

$$\begin{pmatrix}\theta_S(x)\\ n_S(x)\end{pmatrix} \approx \begin{pmatrix}\theta_G(x,z)\\ n_G(x,z)\end{pmatrix}.$$

We now study the phase space of the above system which has the two (z-independent) steady states $S_1 = (\theta_{S_1}(x), n_{S_1}(x))$ and $S_0 = (0,1)$. The system has a propagating pattern solution if and only if there exists a trajectory in the phase space connecting these two steady states. By linearizing about these steady states, one can examine their stability to see whether such a trajectory is possible.

We begin by linearizing about S_1, by setting

$$\theta(x,z) = \theta_S(x) + \tilde{p}(z)\theta_S(x), \tag{4.4a}$$

$$n(x,z) = n_S(x) + \tilde{q}(z)n_S(x), \tag{4.4b}$$

where

$$|\tilde{q}(z)| \ll 1 \quad \text{and} \quad |\tilde{p}(z)| \ll 1.$$

Because of our assumption that the form of the pattern stays fixed while the amplitudes of the propagating patterns change, only the amplitudes of the pattern are perturbed about the steady state.

By substituting (4.4) into (4.1) for the simplified model, that is, with $D = \mu = r = 0$, and dropping the tildes for algebraic convenience, we have the linear system

$$\begin{aligned}
&\left(\frac{\partial^2}{\partial z^2} + 2\frac{\partial^2}{\partial z\partial x} + \frac{\partial^2}{\partial x^2}\right)(p\theta_S)\\
&-\beta\left(\frac{\partial^4}{\partial z^4} + 4\frac{\partial^4}{\partial z^3\partial x} + 6\frac{\partial^4}{\partial z^2\partial x^2} + 4\frac{\partial^4}{\partial z\partial x^3} + \frac{\partial^4 p\theta_S}{\partial x^4}\right)(p\theta_S)\\
&+\left(\frac{\partial^2}{\partial z^2} + \frac{\partial^2}{\partial z\partial x} + \frac{\partial^2}{\partial x^2}\right)(U_1(x)p\theta_S + U_2(x)qn_S) = \rho p\theta_S, \qquad (4.5a)\\
&-v\frac{\partial}{\partial z}(qn_S) = \left(\frac{\partial}{\partial z} + \frac{\partial}{\partial x}\right)\left\{qn_S\left(\frac{\partial}{\partial z} + \frac{\partial}{\partial x}\right)W_0(x)\right.\\
&\qquad\left. + n_S\left(\frac{\partial}{\partial z} + \frac{\partial}{\partial x}\right)(W_1(x)qn_S + W_2(x)p\theta_S)\right\}, \qquad (4.5b)
\end{aligned}$$

where

$$U_1(x) = \frac{2\tau\nu[1+\nu-\nu\theta_S(x)]}{\{[1+\nu-\nu\theta_S(x)]^2 + cn_S^2(x)\}^2},$$

$$U_2(x) = \frac{2\tau n_S(x)[1+\nu-\nu\theta_S(x)]^2}{\{[1+\nu-\nu\theta_S(x)]^2 + cn_S^2(x)\}^2},$$

and

$$W_0(x) = \frac{-\alpha[1-\theta_S(x)]}{1+\gamma n_S(x)},$$
$$W_1(x) = \frac{\alpha\gamma[1-\theta_S(x)]}{[1+\gamma n_S(x)]^2},$$
$$W_2(x) = \frac{\alpha}{1+\gamma n_S(x)}.$$

Likewise, we linearize about the steady state S_0 by setting

$$\theta(x,z) = \tilde{p}(z)\theta_S(x), \tag{4.6a}$$
$$n(x,z) = 1+\tilde{q}(z)n_S(x), \tag{4.6b}$$

where

$$|\tilde{q}(z)| \ll 1 \quad \text{and} \quad |\tilde{p}(z)| \ll 1.$$

Substituting this into (4.1) and dropping the tildes gives

$$\left(\frac{\partial^2}{\partial z^2}+2\frac{\partial^2}{\partial z\partial x}+\frac{\partial^2}{\partial x^2}\right)(p\theta_S)$$
$$-\beta\left(\frac{\partial^4}{\partial z^4}+4\frac{\partial^4}{\partial z^3\partial x}+6\frac{\partial^4}{\partial z^2\partial x^2}+4\frac{\partial^4}{\partial z\partial x^3}+\frac{\partial^4 p\theta_S}{\partial x^4}\right)(p\theta_S)$$
$$+\left(\frac{\partial^2}{\partial z^2}+\frac{\partial^2}{\partial z\partial x}+\frac{\partial^2}{\partial x^2}\right)(P_1 p\theta_S + P_2 q n_S) = \rho p\theta_S, \tag{4.7a}$$
$$-v\frac{\partial}{\partial z}(qn_S) = \left(\frac{\partial^2}{\partial z^2}+2\frac{\partial^2}{\partial z\partial x}+\frac{\partial^2}{\partial x^2}\right)(Q_1 qn_S + Q_2 p\theta_S), \tag{4.7b}$$

where P_1, P_2, Q_1, and Q_2 are as in (2.3).

These linear systems are extremely complicated and it is very difficult to carry out a stability analysis in general because we do not know the functions $\theta_S(x)$ and $n_S(x)$. However, we can approximate these functions in the vicinity of a primary bifurcation from the uniform steady state by using the weakly nonlinear perturbation technique detailed in Appendix B for the case where γ is the bifurcation parameter.

For the purpose of our explanation below we briefly refer back to system (2.1), which is the above set of equations (4.1) written in terms of the space and time coordinates x and t. In section 2 we showed that this system bifurcates from the homogeneous steady state S_0 if the dispersion relation (see (2.2)) becomes positive for some critical eigenvalue k_c^2. This happens, for example, if the bifurcation parameter γ becomes marginally smaller than the critical value γ_c. By setting $\gamma = \gamma_c - \epsilon^2$, where ϵ is the small perturbation parameter, an approximate nonhomogeneous steady state solution for large time (see (2.4)) was found by Cruywagen and Murray (1992) by a multiple time scale analysis (refer to Appendix B of this paper).

The perturbation solution is valid for the traveling coordinate system (4.1) in the region where $z \to -\infty$ and is in fact the steady state solution S_1. Hence, from (2.4), we have that

$$\begin{pmatrix}\theta_{S_1}(x)\\ n_{S_1}(x)\end{pmatrix} = \Lambda\begin{pmatrix}1\\ M\end{pmatrix}(A\cos k_c x + B\sin k_c x) + O(\epsilon^2), \tag{4.8}$$

where the amplitude is given by Λ, M is as in section 2, and $A^2 + B^2$ is given in section 2 and Appendix B.

Next we look at the steady state S_0 as $z \to \infty$ and more specifically at the functions θ_{S_0} and n_{S_0}. Initially, for t very small, the solution of (2.1) evolves from the homogeneous steady state $\theta = 0$, $n = 1$. Since the variables initially take values close to their steady state values we can approximate the nonlinear system by a linearized version about the steady state. The linear solution of (2.1), obtained for large time, can be written as

$$\begin{pmatrix}\theta(x,t)\\ n(x,t)\end{pmatrix} \approx \begin{pmatrix}0\\1\end{pmatrix} + \int_{k_L}^{k_R} p_f(k) \begin{pmatrix}1\\M\end{pmatrix} e^{\lambda(k^2)t}(A\cos kx + B\sin kx)dk,$$

where $p_f(k)$ is determined by a Fourier transform of the initial conditions, A and B are arbitrary constants, M is as before, and $[k_L, k_R]$ is the range of unstable wavenumbers. When performing the weakly nonlinear analysis (see Appendix B) it is assumed that, since we are in the vicinity of the bifurcation point, the linear solution with the critical eigenvalue k_c^2 is the dominant one and, for small enough ϵ, the only one that evolves initially. So, using expressions (4.2) and (4.3) we can write

$$\begin{pmatrix}\theta_{S_0}(x)\\ n_{S_0}(x)\end{pmatrix} = \Lambda \begin{pmatrix}1\\M\end{pmatrix} (A\cos k_c x + B\sin k_c x), \tag{4.9}$$

where we have multiplied the solution by Λ so that the amplitudes of $\theta_{S_0}(x)$ and $n_{S_0}(x)$ are rescaled to be the same as the amplitudes of the final steady state solution (4.8).

Our initial pattern $(\theta_{S_0}(x,z), n_{S_0}(x,z))^T$, far ahead of the leading edge of the traveling wave, is, to $O(\epsilon)$, the same as the final pattern $(\theta_{S_1}(x), n_{S_1}(x))^T$, far behind the wave. This means that our solution $(\theta(x,z), n(x,z))^T$ is, to $O(\epsilon)$, separable in a x-independent part $(p,q)^T$ and a z-independent part $(n_G, \theta_G)^T$.

Hence, to $O(\epsilon)$, we can approximate these functions by

$$\begin{pmatrix}\theta_S\\ n_S\end{pmatrix} = \Lambda \begin{pmatrix}1\\M\end{pmatrix} (A\cos k_c x + B\sin k_c x). \tag{4.10}$$

Substituting this into the linearized system (4.5), ignoring terms of $O(\epsilon^2)$, and equating coefficients of $\cos k_c x$, we get the following two equations:

$$\begin{aligned}&\beta Ap'''' + 4\beta Bp''' - (1 + 6\beta k_c^2 + P_1)Ap'' - (2k_c + 4\beta k_c^3 + P_1 k_c)Bp'\\ &\quad + (k_c^2 + \beta k_c^4 + P_1 k_c^2 + \rho)Ap = MP_2(Aq'' + k_c Bq' - k_c^2 Aq),\end{aligned} \tag{4.11a}$$

$$\begin{aligned}&Q_2 Ap'' + 2Q_2 k_c Bp' - Q_2 Ak_c^2 p = -MQ_1 Aq''\\ &\quad - (vAM + 2MQ_1 k_c B)q' + MQ_1 k_c^2 Aq,\end{aligned} \tag{4.11b}$$

where the prime indicates differentiation with respect to z.

Likewise, by equating coefficients of $\sin k_c x$, we obtain

$$\begin{aligned}&\beta Bp'''' - 4\beta Ap''' - (1 + 6\beta k_c^2 + P_1)Bp'' + (2k_c + 4\beta k_c^3 + P_1 k_c)Ap'\\ &\quad + (k_c^2 - \beta k_c^4 + P_1 k_c^2 - \rho)Bp = MP_2(Bq'' - k_c Aq' - k_c^2 Bq),\end{aligned} \tag{4.12a}$$

$$\begin{aligned}&Q_2 Bp'' - 2Q_2 k_c Ap' - Q_2 Bk_c^2 p = -MQ_1 Bq''\\ &\quad + (vMB + 2MQ_1 k_c A)q' + MQ_1 k_c^2 Bq.\end{aligned} \tag{4.12b}$$

We now add (4.11a) to (4.12a) and (4.11b) to (4.12b) after multiplying (4.11) by A and (4.12) by B. After dividing the two resulting equations by $(A^2 + B^2)$ we are left with

$$\begin{aligned} &\beta p'''' - (1 + 6\beta k_c^2 + P_1)p'' \\ &+ (k_c^2 + \beta k_c^4 + P_1 k_c^2 + \rho)p = MP_2(q' - k_c^2 q), \end{aligned} \tag{4.13a}$$

$$Q_2 p'' - Q_2 k_c^2 p = -MQ_1 q'' + vMq' + MQ_1 k_c^2 q, \tag{4.13b}$$

which is the linearized system about the steady state S_1 to $O(\epsilon)$.

The linearized system to $O(\epsilon)$ about the steady state S_0 can be found in a similar fashion. We substitute (4.10) and (4.9) into (4.7), follow the same procedure as above, and find that the linearized system about S_0 is exactly the same as the system (4.13). The complexity of the two original linear systems has now been reduced considerably—they are dependent only on the variable z and are written in terms of the envelope functions p and q.

By setting

$$p_0 = p, \qquad p_1 = p', \qquad p_2 = p'', \qquad p_3 = p''', \qquad q_0 = q, \qquad q_1 = q',$$

the coupled pair of ordinary differential equations (4.13) can be written as a sixth-order system, namely,

$$\begin{aligned} p_0' &= p_1, \\ p_1' &= p_2, \\ p_2' &= p_3, \\ p_3' &= \frac{1}{\beta}\left[\left(-\beta k_c^4 - (P_1 + 1 - \frac{P_2 Q_2}{Q_1})k_c^2 - \rho\right)p_0\right. \\ &\qquad \left. + \left(6\beta k_c^2 + P_1 + 1 - \frac{P_2 Q_2}{Q_1}\right)p_2 + \frac{P_2 Q_2 v}{Q_1^2} q_1\right], \\ q_0' &= q_1, \\ q_1' &= p_2 - k_c^2 - \frac{v}{Q_1} q_1 + k_c^2 q_0. \end{aligned}$$

We examine the stability of this system in the usual way by looking for solutions of the form

$$(p_0, p_1, p_2, p_3, q_0, q_1)^T = \boldsymbol{W} e^{\eta z}, \tag{4.14}$$

where the vector $\boldsymbol{W}$ is constant and the sign of $\Re\eta$ determines the stability of the steady state.

Substituting (4.14) into the linearized system of equations leads to a system of six homogeneous equations. A nontrivial solution exists for this system if and only if η satisfies the following solvability condition:

$$\begin{aligned} \Delta(\eta) &= \eta^6 + \frac{v}{Q_1}\eta^5 - \left(k_c + \frac{\chi}{\beta}\right)\eta^4 - \frac{v}{\beta Q_1}\left(6\beta k_c^2 + P_1 + 1\right)\eta^3 \\ &+ \frac{1}{\beta}\left(k_c^2 \chi - \omega\right)\eta^2 + \frac{1}{\beta Q_1}\left(\beta k_c^4 + k_c^2 + P_1 k_c^2 + \rho\right)\eta + \frac{k_c^2 \omega}{\beta} = 0, \end{aligned} \tag{4.15}$$

where

$$\chi = 6\beta k_c^2 + P_1 + 1 - \frac{P_2 Q_2}{Q_1}$$

and

$$\omega = -\beta k_c^4 - P_1 k_c^2 + \frac{P_2 Q_2 k_c^2}{Q_1} - k_c^2 - \rho.$$

From the linear analysis of section 2

$$\beta Q_1(\gamma) k_c^6 - [P_2 Q_2(\gamma) - P_1 Q_1(\gamma) - Q_1(\gamma)] k_c^4 + \rho Q_1(\gamma) k_c^2 < 0 \quad \text{if} \quad \gamma < \gamma_c,$$

and so

$$\omega(\gamma) > 0 \quad \text{if} \quad \gamma < \gamma_c.$$

Furthermore,

$$P_2 Q_2(\gamma) - P_1 Q_1(\gamma) - Q_1(\gamma) > 0 \quad \text{if} \quad \gamma < \gamma_c,$$

(see Appendix B) and thus

$$\chi(\gamma) - 6\beta k_c^2 > 0 \quad \text{if} \quad \gamma < \gamma_c.$$

Using this we have that

$$k_c^2 \chi - \omega = 3\beta k_c^2 + \rho + 2k_c^2(\chi - 4\beta k_c^2) > 0 \quad \text{if} \quad \gamma < \gamma_c.$$

Hence the polynomial (4.15) has only two sign changes in the sequence of coefficients and Descartes' rule of signs implies that there are either two or zero positive roots. By substituting $-\eta$ for η into (4.15) we see that the resulting polynomial has four sign changes and it therefore has either four, two, or zero negative roots.

As z changes from $-\infty$ to ∞ the traveling envelope corresponds to a trajectory connecting S_1 to S_0 in phase space. As necessary conditions for such a trajectory to exist, an unstable manifold at S_1 and a stable manifold at S_0 are required. The solvability condition (4.15), which is valid to $O(\epsilon)$ at both steady states, allows for both stable and unstable manifolds. Notice, however, that these are not sufficient conditions; whether there indeed exists a trajectory connecting the steady state S_1 to S_0 cannot be proven in general.

5. Applying the envelope method. Here we consider a specific example to illustrate how the envelope method can be used to predict the wave speed of the propagating patterns. We chose the parameter set given in section 3 and set $\epsilon = 0.01$ so that we are in the vicinity of the bifurcation point. For this parameter set, the polynomial (4.15) has two positive and two negative roots for all $v \geq 0$ and hence we have at least a two-dimensional stable manifold and a two-dimensional unstable manifold. This suggests that a trajectory from S_1 to S_0 is possible for any speed $v \geq 0$. This is inconsistent with the numerical results of section 3 which show that the solution propagates at a fixed wave speed depending on the parameter set chosen.

Closer inspection of (4.15) reveals that, for this parameter set, two more negative eigenvalues appear as the parameter v increases. If we hypothesize that the stable manifold at S_0, into which the connecting trajectory shoots, is represented by these

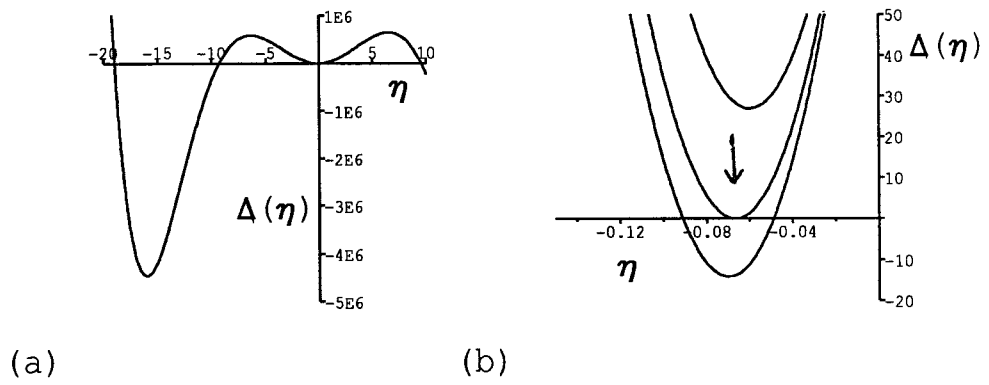

FIG. 3. *The solvability condition* (4.15) *with parameter values as in section* 3 *and* $\epsilon = 0.01$. (a) *All the roots of the polynomial are shown.* (b) *The double root that appears as the wave speed* v *increases through* 0.13.

TABLE 1

A comparison of the wave speeds obtained for the propagating pattern from the asymptotic method, the envelope method, and the numerical simulations.

ϵ	Numerical result	Envelope method	Asymptotic method
0.01	0.13	0.13	0.13
0.1	1.35	1.33	1.36
0.5	9.4	-	9.9

two roots, we can get a bound on v. One can find the minimum value of v, for which these two new roots appear as a double negative root. This value of v would then represent a lower bound on the wave speed of the traveling pattern. Although we cannot prove the existence of a trajectory connecting the steady states S_0 and S_1, such a trajectory seems highly likely in light of the numerical experiments performed below.

Numerically we found that the double negative root appeared at a minimum value of $v = 0.13$ (see Figure 3). The actual speed at which the pattern propagates, as was found from the numerical simulations, agrees exactly with this prediction. As is the case for the Fisher wave (see, for example, Murray (1989)) we see that our wave of pattern formation indeed travels at, or very close to, the minimum speed, since it agrees well with the analytical approximation for the minimum speed.

If we choose $\epsilon = 0.1$, our analytical approximation of $v = 1.33$ compares favorably with the actual numerically computed speed of 1.35. However, if we move still further away from the bifurcation point, this method breaks down, as one would expect (see Table 1 for a summary of the results).

Extensive numerical simulations show that this method works well. To test the general applicability of this envelope method for determining the minimum wave speed at which waves of pattern formation travel, we applied the method to a reaction-diffusion system. For the purpose of our analysis we chose the Schnakenberg system, one of the simplest reaction-diffusion systems (see Schnakenberg (1979)). Instead of

a sixth-order polynomial we found, as stability condition for the two steady states, a fourth-order polynomial. As we varied the wave speed we got either zero or two stable manifolds at these steady states. Therefore if a trajectory connecting the two steady states does exist a bound on the wave speed is obtained. The numerically computed traveling wave speed compared favorably with the minimum wave speed predicted analytically.

6. Conclusion. We have proposed a new "envelope" method for calculating the speed of propagating patterns in a one-dimensional domain, arising from typical biological pattern formation models such as reaction-diffusion and mechanochemical equations. As a specific example of a pattern formation system, we have considered the tissue interaction model of Cruywagen and Murray (1992). Extensive numerical simulations show that, in the vicinity of a primary bifurcation point, the spatially varying steady state patterns forming far behind the advancing front of pattern are very similar to those developing at the leading edge, the most notable difference being in the amplitude of the spatially periodic patterns. We track the change in amplitude by plotting the envelope function which is a traveling wave propagating with constant speed. By transforming to traveling wave coordinates we conjecture that the speed of propagation is bounded below by the critical value of the speed v at which two of the eigenvalues in the linearization change from being complex to being real via a double root (Figure 3(b)).

In the classical Fisher model (Fisher (1937)), the system in traveling wave coordinates is a pair of coupled ordinary differential equations with two steady states. The minimum wave speed is at the critical value of v at which one of the steady states changes from a stable node to a stable spiral. It can be rigorously shown that a trajectory corresponding to a saddle-node connection exists for wave speeds above this minimum value. Moreover, any initial conditions with compact support will evolve into a wave traveling with this minimum wave speed (see, for example, Murray (1989)).

In this paper, our model system is a six-dimensional phase space and therefore one cannot derive such rigorous results. Our numerical simulations suggest, however, that the phenomenon of a minimum wave speed holds here as well. Due to the basic assumptions underpinning the envelope method, it has a high degree of accuracy in the vicinity of a bifurcation point but fails as one moves a substantial distance away from the bifurcation point. We have tested other models (for example, reaction-diffusion models) and found that they too give results consistent with the above conjecture.

The envelope method is more generally applicable than the alternative asymptotic method proposed by Murray and Myerscough (1992) and mentioned in the introduction of this paper. The asymptotic method is based on a quadratic approximation of the dispersion relation. The accuracy with which the caricature dispersion relation approximates the full dispersion relation has an important effect on the accuracy of the wave speed predicted by the asymptotic method. Moreover, in their approach it is unclear exactly how each parameter influences the wave speed as these do not appear in the caricature dispersion relation. Thus, one cannot directly relate parameters in the caricature dispersion relation to actual model parameters. This contrasts with the envelope method in which we can examine the effect that varying a particular parameter has on the dispersion relation and thus how it influences the wave speed.

Appendix A. Here we briefly describe the tissue-interaction model. The reader is referred to Cruywagen and Murray (1992) for the full details of the derivation of the model.

The model assumes that tissue interaction between the epithelial and dermal skin layers is mediated by two signal chemicals which are secreted in each layer, respectively. These chemicals diffuse across the basal lamina—a thin sheet separating the dermis and epidermis—thus transferring *information* between the layers.

The model consists of seven equations: four to describe the production, degradation, and diffusion of the chemicals within and between layers; two conservation equations for the dermal and epidermal cell densities, respectively; and finally, a force balance equation for modeling stresses in the epithelium. As the chemical equations are standard, we shall not describe them here, but will instead focus on the force balance and cell density equations.

The epithelium is modeled as a viscoelastic continuum at a low Reynolds number in which active traction forces exerted by the epidermal cells are balanced by elastic restoring forces and external elastic tethering to the basal lamina. The force balance equation has the form

$$\nabla \cdot \left\{ \overbrace{\frac{E}{1+\upsilon}\left[\boldsymbol{\varepsilon} - \beta_1 \nabla^2 \boldsymbol{\varepsilon} + \frac{\upsilon}{1-2\upsilon}(\theta - \beta_2 \nabla^2 \theta)\boldsymbol{I}\right]}^{\text{elastic stress}} \right.$$

$$\left. + \overbrace{\mu_1 \frac{\partial \boldsymbol{\varepsilon}}{\partial t} + \mu_2 \frac{\partial \theta}{\partial t}\boldsymbol{I}}^{\text{viscous stress}} + \overbrace{\frac{\tau s^2}{1+cs^2}\boldsymbol{I}}^{\text{traction stress}} \right\} = \overbrace{\rho \boldsymbol{u}}^{\text{body forces}}, \tag{A.1}$$

where $\boldsymbol{u}(\boldsymbol{x}, t)$ is the displacement at time t of a material point in the epithelium which was initially at position $\boldsymbol{x}$, $\theta = \nabla \cdot \boldsymbol{u}$ is the dilation, $\boldsymbol{\varepsilon} = \frac{1}{2}(\nabla \boldsymbol{u} + \nabla \boldsymbol{u}^T)$ is the strain tensor, where T denotes the transpose, and $s(\boldsymbol{x}, t)$ is the concentration of the signal chemical produced in the dermis. The parameters E and υ are Young's modulus and Poisson's ratio, respectively, while μ_1 and μ_2 are the shear and bulk viscosities, respectively, $\boldsymbol{I}$ is the unit tensor, and β_1 and β_2 reflect long-range elastic stresses (see Murray (1989)). The traction stress is a switch function of the dermal signal chemical, s, with τ measuring the magnitude and c the abruptness of the switch.

We assume that the epidermal cells migrate due to convection only. Hence the epidermal cell density $N(\boldsymbol{x}, t)$ satisfies the conservation equation

$$\frac{\partial N}{\partial t} = \overbrace{-\nabla \cdot N \frac{\partial \boldsymbol{u}}{\partial t}}^{\text{convection}}. \tag{A.2}$$

The conservation equation for dermal cell density, $n(\boldsymbol{x}, t)$, accounts for diffusion, mitosis, and chemotaxis toward the signal chemical produced in the epithelium. Hence, the dermal chemotaxis equation is

$$\frac{\partial n}{\partial t} = \overbrace{D\nabla^2 n}^{\text{diffusion}} - \overbrace{\alpha \nabla \cdot n \nabla e}^{\text{chemotaxis}} + \overbrace{rn(\bar{n} - n)}^{\text{cell growth}}, \tag{A.3}$$

where D is the coefficient of diffusion, α is the chemotactic coefficient, $e(\boldsymbol{x}, t)$ is the concentration of the signal chemical produced in the epithelium, and r and $\bar{n}$ are positive constants.

We can linearize about the uniform epidermal cell density steady state, say $\hat{N}$, and integrate (A.2) to obtain a linear relationship between N and θ, namely, $N = \hat{N}(1-\theta)$. Using this and assuming that the chemical kinetics occur on a fast timescale, one can find actual algebraic expressions for the signal chemicals in terms of θ and n, namely, $s = n/(1+\nu(1-\theta))$ and $e = (1-\theta)/(1+\gamma n)$ (see Cruywagen and Murray (1992) for full details). From these expressions we observe that the active traction stress in the epidermis is induced by high concentrations of dermal cells, but inhibited by high concentrations of epithelial cells. Similarly, dermal chemotaxis occurs toward high concentrations of epithelial cells but is inhibited by high concentrations of dermal cells.

The simplified nondimensionalised set of equations is shown in section 2, equation (2.1), for one spatial dimension.

Appendix B. Here we examine the time evolution of the nonlinear system (2.1) using a multiscale perturbation procedure on a one-dimensional domain. This shows how the different parameters are involved in determining the amplitude of the pattern and gives conditions under which a steady state spatial pattern is attained. Refer to Cruywagen and Murray (1992) for further details and to Cruywagen, Maini, and Murray (1997) for the two-dimensional version of this analysis.

We are interested in the simplest biologically realistic version of the basic tissue interaction model for which we can isolate any unstable wavenumber with an appropriate parameter combination. We assume that $D = 0$, $r = 0$, and $\mu = 0$ in (2.1). The one-dimensional version of the reduced model is then

$$\frac{\partial^2\theta}{\partial x^2} - \beta\frac{\partial^4\theta}{\partial x^4} + \tau\frac{\partial^2}{\partial x^2}\frac{n^2}{[1+\nu(1-\theta)]^2+cn^2} = \rho\theta, \tag{B.1a}$$

$$\frac{\partial n}{\partial t} = -\alpha\frac{\partial}{\partial x}\left\{n\frac{\partial}{\partial x}\left(\frac{1-\theta}{1+\gamma n}\right)\right\}. \tag{B.1b}$$

This system has the parabolic-type dispersion relation

$$\lambda(k^2) = -\frac{\beta Q_1 k^6 - (P_2Q_2 - P_1Q_1 - Q_1)k^4 + \rho Q_1 k^2}{\beta k^4 + (P_1+1)k^2 + \rho}; \tag{B.2}$$

(refer to (2.2)). Since $\lim_{\gamma\to 0^+} Q_1(\gamma) = 0$ and $\lim_{\gamma\to 0^+} Q_2(\gamma) = \alpha$, we can force the dispersion relation to be positive by ensuring that γ is small enough. It is easy to show that if $P_2Q_2(\gamma) - P_1Q_1(\gamma) - Q_1(\gamma) > 0$, then the uniform steady state loses stability as γ decreases beyond a critical value γ_c, where

$$(P_2Q_2(\gamma_c) - P_1Q_1(\gamma_c) - Q_1(\gamma_c))^2 = 4\beta\rho Q_1^2(\gamma_c).$$

The corresponding critical wavenumber is

$$k_c^2 = \frac{P_2Q_2(\gamma_c) - P_1Q_1(\gamma_c) - Q_1(\gamma_c)}{2\beta Q_1(\gamma_c)}. \tag{B.3}$$

The epithelial and dermal cell condensations which form during early chick skin morphogenesis are small; we therefore hypothesize that they occur in the vicinity of the bifurcation point. We shall also assume that there is one and only one wavenumber k that has a positive growth rate. Furthermore, we assume that at bifurcation $k = k_c$, and that the solutions are periodic in space with period $2\pi/k_c$.

As the linear growth rate is small we look, as usual, for solutions that evolve on the slow time scale $\epsilon^2 t$; thus we set

$$\gamma = \gamma_c - \epsilon^2, \quad \text{where } 0 < \epsilon \ll 1, \quad \text{and } T = \epsilon^2 t. \tag{B.4}$$

We consider the variables θ and n as functions of ϵ, x, and T, ignoring the t dependence except through T in the usual way. We assume power series expansions for θ and n,

$$\theta(x, T, \epsilon) = \epsilon\theta_1(x, T) + \epsilon^2\theta_2(x, T) + \cdots, \tag{B.5a}$$

$$n(x, T, \epsilon) = 1 + \epsilon n_1(x, T) + \epsilon^2 n_2(x, T) + \cdots. \tag{B.5b}$$

By substituting (B.4) and (B.5) into (B.1) we reduce the analysis of the nonlinear system to that of a hierarchy of linear equations by equating coefficients of $O(\epsilon)$, $O(\epsilon^2)$, and so on.

To $O(\epsilon)$ we have

$$\mathcal{L}\begin{pmatrix}\theta_1\\ n_1\end{pmatrix} = \mathbf{0},$$

where

$$\mathcal{L} \equiv \begin{pmatrix} -\beta\frac{\partial^4}{\partial x^4} + (1+P_1)\frac{\partial^2}{\partial x^2} - \rho & P_2\frac{\partial^2}{\partial x^2} \\ Q_2\frac{\partial^2}{\partial x^2} & Q_1\frac{\partial^2}{\partial x^2}\end{pmatrix}.$$

Thus we have

$$\begin{pmatrix}\theta_1\\ n_1\end{pmatrix} = \begin{pmatrix}1\\ M\end{pmatrix}\left(A(T)\cos k_c x + B(T)\sin k_c x\right),$$

with M as in (2.4).

In the usual way, $A(T)$ and $B(T)$ are determined by suppressing secular terms later. Secular terms appear at $O(\epsilon^3)$, where we have

$$\mathcal{L}\begin{pmatrix}\theta_3\\ n_3\end{pmatrix} = \begin{pmatrix}R_1\\ R_2\end{pmatrix}, \tag{B.6}$$

where R_1 and R_2 are known functions of θ_1, θ_2, n_1, and n_2 (where θ_2 and n_2 are determined from the equations at $O(\epsilon^2)$). Secular terms appear in the solutions for $(\theta_3, n_3)^T$. To suppress these secular terms we use the Fredholm alternative (see, for example, Keener (1988)). A solution $\mathbf{w} = (\theta_3, n_3)^T$ exists for (B.6) if and only if the Fredholm alternative is satisfied, that is, the inner product

$$\langle \mathbf{w}^*, \mathbf{R}\rangle = \int_0^{\frac{2\pi}{k_c}} (\theta^*\bar{R}_1 + n^*\bar{R}_2)\, dx = 0,$$

where the bar denotes the complex conjugate and $\mathbf{w}^*$ is a bounded solution of the adjoint problem

$$\mathcal{L}^*(\mathbf{w}^*) = \mathbf{0},$$

where $\mathcal{L}^*$ is the adjoint operator to $\mathcal{L}$.

Solving this gives, after much tedious algebra, the Landau equation for the evolution of the amplitude $A^2(T) + B^2(T)$ on the slow time scale as

$$\frac{1}{2}\frac{d\left(A^2+B^2\right)}{dT} = \Omega\left(A^2+B^2\right) + \Gamma\left(A^2+B^2\right)^2, \tag{B.7}$$

where

$$\Omega = \frac{\gamma k_c^2}{(\gamma_c+1)^3} > 0$$

and Γ is a complicated expression of the model parameters (refer to Cruywagen and Murray (1992)).

The behavior of this equation is summarized in Cruywagen and Murray (1992). If $\Gamma < 0$ the solution evolves to

$$\begin{pmatrix}\theta\\ n\end{pmatrix} = \begin{pmatrix}0\\ 1\end{pmatrix} + \epsilon\left(A\cos k_c x + B\sin k_c x\right) + O(\epsilon^2) \text{ as } T\to\infty, \tag{B.8}$$

where $A^2 + B^2 = -\Omega/\Gamma$.

Acknowledgments. The authors thank Dr. Peter Grindrod for valuable comments and ideas regarding the envelope method. G. C. C. Cruywagen would like to thank the South African Foundation for Research Development for its financial support. P. K. M. Maini would like to thank the Department of Mathematics of Williams College, Massachusetts, for its hospitality and support.

REFERENCES

G. C. Cruywagen, P. K. Maini, and J. D. Murray (1992), *Sequential pattern formation in a model for skin morphogenesis*, IMA J. Math. Appl. Med. Biol., 9, pp. 227–248.

G. C. Cruywagen and J. D. Murray (1992), *On a tissue interaction model for skin pattern formation*, J. Nonlinear Sci., 2, pp. 217–240.

G. C. Cruywagen, P. K. Maini, and J. D. Murray (1994), *Travelling waves in a tissue interaction model for skin pattern formation*, J. Math. Biol., 33, pp. 193–216.

G. C. Cruywagen, P. K. Maini, and J. D. Murray (1997), *Biological pattern formation in two-dimensional spatial domains: A nonlinear bifurcation analysis*, SIAM J. Appl. Math., 57, pp. 1485–1509.

D. Davidson (1983a), *The mechanism of feather pattern development in the chick.* I. *The time determination of feather position*, J. Embryol. Exp. Morph., 74, pp. 245–259.

D. Davidson (1983b), *The mechanism of feather pattern development in the chick.* II. *Control of the sequence of pattern formation*, J. Embryol. Exp. Morph., 74, pp. 261–273.

R. A. Fisher (1937), *The wave of advance of advantageous genes*, An. Eugenics, 7, pp. 353–369.

J. P. Keener (1988), *Principles of Applied Mathematics, Transformation and Approximation*, Addison-Wesley, Reading, MA.

A. Kolmogoroff, I. Patrovsky, and N. Piscounoff (1937), *Étude de l'équation de la diffusion avec croissance de la quantité de matière et son application à un problème biologique*, Moscow Univ. Bull. Math., 1, pp. 1–25.

P. F. A. Maderson (1965a), *The embryonic development of the squamate integument*, Acta Zool., 46, pp. 275–295.

P. F. A. Maderson (1965b), *The structure and development of the squamate epidermis*, in Symposium on the Biology of the Skin and Hair Growth, A. G. Lyne and B. F. Short, eds., Angus and Robertson, Sydney, 1965, pp. 129–153.

P. K. Maini, ed. (1995), *Travelling waves in biology, chemistry, ecology and medicine, Part* 1, FORMA Special Issue, 10, pp. 145–280.

P. K. Maini, ed. (1996), *Travelling waves in biology, chemistry, ecology and medicine, Part* 2, FORMA Special Issue, 11, pp. 1–80.

J. D. Murray, *Mathematical Biology*, Springer–Verlag, Heidelberg, 1989.

J. D. Murray and G. C. Cruywagen (1994), *Threshold bifurcation in tissue interaction models for spatial pattern generation*, Philos. Trans. Roy. Soc. London Ser. A, 347, pp. 661–676.

J. D. Murray, G. C. Cruywagen, and P. K. Maini, *Pattern formation in tissue interaction models*, in Frontiers in Mathematical Biology, S. Levin, ed., Lecture Notes in Biomath. 100, Springer–Verlag, Heidelberg, 1994, pp. 104–116.

J. D. Murray, D. C. Deeming, and M. W. J. Ferguson (1990), *Size dependent pigmentation pattern formation in embryos of Alligator Mississipiensis: Time of initiation of pattern generation mechanism*, Proc. Roy. Soc. London B, 239, pp. 279–293.

M. R. Myerscough and J. D. Murray (1992), *Analysis of propagating pattern in a chemotaxis system*, Bull. Math. Biol., 54, pp. 77–94.

M. Pearson and T. Elsdale (1979), *Somitogenesis in amphibian embryos.* I. *Experimental evidence for an interaction between two temporal factors in the specification of the somite pattern*, J. Embryol. Exp. Morph., 51, pp. 27–50.

J. Schnakenberg (1979), *Simple chemical reaction systems with limit cycle behaviour*, J. Theor. Biol., 81, pp. 389–400.

E. C. Zeeman (1974), *Primary and secondary waves in developmental biology*, in Some Mathematical Questions in Biology, VI, Lectures Math. Life Sci. 74, Amer. Math. Soc., Providence, RI, 1974, pp. 69–161.